An adaptive filter for studying the life cycle of optical rogue waves

Chu Liu[1, 2, 4], Eric J. Rees[2, 4], Toni Laurila[2], Shuisheng Jian[1], and Clemens F. Kaminski [2, 3,*]

[1]*Institute of Lightwave Technology, Key Lab of All Optical Network and Advanced Telecommunication Network of EMC, Beijing Jiaotong University, Beijing 100044, China*
[2]*Department of Chemical Engineering and Biotechnology, University of Cambridge, Pembroke Street, CB2 3RA, UK*
[3]*SAOT School of Advanced Optical Technologies, Friedrich Alexander University, D-91058 Erlangen, Germany*
[4]*These authors contributed equally to this work*
**cfk23@cam.ac.uk*

Abstract: We present an adaptive numerical filter for analyzing fiber-length dependent properties of optical rogue waves, which are highly intense and extremely red-shifted solitons that arise during supercontinuum generation in photonic crystal fiber. We use this filter to study a data set of 1000 simulated supercontinuum pulses, produced from 5 ps pump pulses containing random noise. Optical rogue waves arise in different supercontinuum pulses at various positions along the fiber, and exhibit a lifecycle: their intensity peaks over a finite range of fiber length before declining slowly.

OCIS codes: (060.5530) Fiber optics and optical communications: Pulse propagation and temporal solitons; (190.4370) Nonlinear optics: Nonlinear optics, fibers.

References and links

1. J. M. Dudley, and J. R. Taylor, Supercontinuum Generation in Optical Fibers, (Cambridge University Press, Cambridge, 2010)
2. J. M. Dudley, G. Genty, and S. Coen, "Supercontinuum generation in photonic crystal fiber," Rev. Mod. Phys. **78**(4), 1135–1184 (2006).
3. J. K. Ranka, R. S. Windeler, and A. J. Stentz, "Visible continuum generation in air-silica microstructure optical fibers with anomalous dispersion at 800 nm," Opt. Lett. **25**(1), 25–27 (2000).
4. P. Russell, "Photonic crystal fibers," Science **299**(5605), 358–362 (2003).
5. T. Udem, R. Holzwarth, and T. W. Hänsch, "Optical frequency metrology," Nature **416**(6877), 233–237 (2002).
6. J. Hult, R. S. Watt, and C. F. Kaminski, "Dispersion measurement in optical fibers using supercontinuum pulses," J. Lightwave Technol. **25**(3), 820–824 (2007).
7. M. Schnippering, P. R. Unwin, J. Hult, T. Laurila, C. F. Kaminski, J. M. Langridge, R. L. Jones, M. Mazurenka, and S. R. Mackenzie, "Evanescent wave broadband cavity enhanced absorption spectroscopy using supercontinuum radiation: A new probe of electrochemical processes," Electrochem. Commun. **10**(12), 1827–1830 (2008).
8. L. van der Sneppen, G. Hancock, C. F. Kaminski, T. Laurila, S. R. Mackenzie, S. R. T. Neil, R. Peverall, G. A. D. Ritchie, M. Schnippering, and P. R. Unwin, "Following interfacial kinetics in real time using broadband evanescent wave cavity-enhanced absorption spectroscopy: a comparison of light-emitting diodes and supercontinuum sources," Analyst (Lond.) **135**(1), 133–139 (2009).
9. C. F. Kaminski, R. S. Watt, A. D. Elder, J. H. Frank and J. Hult, "Supercontinuum radiation for application in chemical sensing and microscopy," Appl. Phys. B **92**(3), 367–378 (2008).
10. J. Hult, R. S. Watt, and C. F. Kaminski, "High bandwidth absorption spectroscopy with a dispersed supercontinuum source," Opt. Express **15**(18), 11385–11395 (2007), http://www.opticsinfobase.org/abstract.cfm?URI=oe-15-18-11385.
11. J. M. Langridge, T. Laurila, R. S. Watt, R. L. Jones, C. F. Kaminski, and J. Hult, "Cavity enhanced absorption spectroscopy of multiple trace gas species using a supercontinuum radiation source," Opt. Express **16**(14), 10178–10188 (2008), http://www.opticsinfobase.org/abstract.cfm?URI=OE-16-14-10178.
12. R. S. Watt, T. K. Laurila, C. F. Kaminski, and J. F. Hult, "Cavity enhanced spectroscopy of high-temperature $H_{(2)}o$ in the near-infrared using a supercontinuum light source," Appl. Spectrosc. **63**(12), 1389–1395 (2009).
13. S. Smirnov, J. D. Ania-Castanon, T. J. Ellingham, S. M. Kobtsev, S. Kukarin, and S. K. Turitsyn, "Optical spectral broadening and supercontinuum generation in telecom applications," Opt. Fiber Technol. **12**(2), 122–147 (2006).

#136335 - $15.00 USD Received 8 Oct 2010; revised 19 Nov 2010; accepted 19 Nov 2010; published 30 Nov 2010

14. S. Schlachter, S. Schwedler, A. Esposito, G. S. Kaminski Schierle, G. D. Moggridge, and C. F. Kaminski, "A method to unmix multiple fluorophores in microscopy images with minimal a priori information," Opt. Express **17**(25), 22747–22760 (2009), http://www.opticsinfobase.org/VJBO/abstract.cfm?URI=oe-17-25-22747.
15. J. H. Frank, A. D. Elder, J. Swartling, A. R. Venkitaraman, A. D. Jeyasekharan, and C. F. Kaminski, "A white light confocal microscope for spectrally resolved multidimensional imaging," J. Microsc. **227**(3), 203–215 (2007).
16. D. R. Solli, C. Ropers, P. Koonath, and B. Jalali, "Optical rogue waves," Nature **450**(7172), 1054–1057 (2007).
17. D. R. Solli, C. Ropers, and B. Jalali, "Active control of rogue waves for stimulated supercontinuum generation," Phys. Rev. Lett. **101**(23), 233902 (2008).
18. J. M. Dudley, G. Genty, and B. J. Eggleton, "Harnessing and control of optical rogue waves in supercontinuum generation," Opt. Express **16**(6), 3644–3651 (2008), http://www.opticsinfobase.org/abstract.cfm?URI=OE-16-6-3644.
19. G. Genty, C. M. de Sterke, O. Bang, F. Dias, N. Akhmediev, and J. M. Dudley, "Collisions and turbulence in optical rogue wave formation," Phys. Lett. A **374**(7), 989–996 (2010).
20. M. Erkintalo, G. Genty, and J. M. Dudley, "Rogue-wave-like characteristics in femtosecond supercontinuum generation," Opt. Lett. **34**(16), 2468–2470 (2009).
21. A. Mussot, A. Kudlinski, M. Kolobov, E. Louvergneaux, M. Douay, and M. Taki, "Observation of extreme temporal events in CW-pumped supercontinuum," Opt. Express **17**(19), 17010–17015 (2009), http://www.opticsinfobase.org/abstract.cfm?URI=oe-17-19-17010.
22. C. Lafargue, J. Bolger, G. Genty, F. Dias, J. M. Dudley, and B. J. Eggleton, "Direct detection of optical rogue wave energy statistics in supercontinuum generation," Electron. Lett. **45**(4), 217–218 (2009).
23. K. Hammani, C. Finot, J. M. Dudley, and G. Millot, "Optical rogue-wave-like extreme value fluctuations in fiber Raman amplifiers," Opt. Express **16**(21), 16467–16474 (2008), http://www.opticsinfobase.org/abstract.cfm?URI=oe-16-21-16467.
24. N. Akhmediev, J. Soto-Crespo, and A. Ankiewicz, "Extreme waves that appear from nowhere: On the nature of rogue waves," Phys. Lett. A **373**(25), 2137–2145 (2009).
25. A. Aalto, G. Genty, and J. Toivonen, "Extreme-value statistics in supercontinuum generation by cascaded stimulated Raman scattering," Opt. Express **18**(2), 1234–1239 (2010), http://www.opticsinfobase.org/abstract.cfm?URI=oe-18-2-1234.
26. M. Taki, A. Mussot, A. Kudlinski, M. Kolobov, E. Louvergneaux, and M. Douay, "Third-order dispersion for generating optical rogue solitons," Phys. Lett. **374**(4), 691–695 (2010).
27. G. Genty, S. Coen, and J. M. Dudley, "Fiber supercontinuum sources (Invited)," J. Opt. Soc. Am. B **24**(8), 1771–1785 (2007).
28. J. M. Dudley, G. Genty, F. Dias, B. Kibler, and N. Akhmediev, "Modulation instability, Akhmediev Breathers and continuous wave supercontinuum generation," Opt. Express **17**(24), 21497–21508 (2009), http://www.opticsinfobase.org/abstract.cfm?URI=oe-17-24-21497.
29. A. V. Gorbach, and D. V. Skryabin, "Light trapping in gravity-like potentials and expansion of supercontinuum spectra in photonic-crystal fibres," Nat. Photonics **1**(11), 653–657 (2007).
30. A. V. Gorbach, and D. V. Skryabin, "Theory of radiation trapping by the accelerating solitons in optical fibers," Phys. Rev. A **76**(5), 053803 (2007).
31. D. R. Solli, C. Ropers, and B. Jalali, "Rare frustration of optical supercontinuum generation," Appl. Phys. Lett. **96**(15), 151108 (2010).
32. G. P. Agrawal, *Nonlinear Fiber Optics*, 4th ed. (Academic, San Diego, 2007).
33. J. Hult, "A fourth-order Runge-Kutta in the interaction picture method for simulating supercontinuum generation in optical fibers," J. Lightwave Technol. **25**(12), 3770–3775 (2007).
34. A. M. Heidt, "Efficient adaptive step size method for the simulation of supercontinuum generation in optical fibers," J. Lightwave Technol. **27**(18), 3984–3991 (2009).
35. S. M. Kobtsev, and S. V. Smirnov, "Modelling of high-power supercontinuum generation in highly nonlinear, dispersion shifted fibers at CW pump," Opt. Express **13**(18), 6912–6918 (2005), http://www.opticsinfobase.org/oe/abstract.cfm?uri=oe-13-18-6912.
36. Q. Lin, and G. P. Agrawal, "Raman response function for silica fibers," Opt. Lett. **31**(21), 3086–3088 (2006).
37. F. Luan, D. V. Skryabin, A. V. Yulin, and J. C. Knight, "Energy exchange between colliding solitons in photonic crystal fiber," Opt. Express **14**(21), 9844–9853 (2006), http://www.opticsinfobase.org/oe/abstract.cfm?uri=oe-14-21-9844.

1. Introduction

Supercontinuum (SC) light, generated by propagating intense laser pulses along photonic crystal fiber (PCF) [1–4], has attracted interest for many applications including frequency metrology [5,6], spectroscopy [7–12], telecommunications [13] and microscopy [14,15]. Such applications demand wide spectral coverage together with good stability and low noise. An interesting challenge to these aspects of SC generation is posed by optical rogue waves. Optical rogue waves (also called rogue solitons, RS) are packets of extremely intense and red-shifted light that can arise during the propagation of laser light along nonlinear optical fiber

#136335 - $15.00 USD Received 8 Oct 2010; revised 19 Nov 2010; accepted 19 Nov 2010; published 30 Nov 2010

[16–21]. They are rare, but striking because of their high intensity, extreme spectral shift and time-delay, with implications for light source stability and fiber damage.

The properties of RS have been studied by experiment and numerical models [16–26]. When SC light is generated from long pump pulses, the initial phase of propagation involves modulation instability which can be interpreted as the growth of Akhmediev breather structures [27,28]. This leads to a regime of turbulent collisions, in which further effects such as Raman scattering and dispersive wave trapping give rise to the broad supercontinuum spectrum [29,30]. Occasionally, dependent on the spontaneous input noise, the turbulent regime gives rise to a very intense soliton – an optical rogue soliton [19]. Previous studies have found that modulation of the initial laser pulse can increase the abundance of RS [18]. Alternatively, formation of RS can be suppressed by tailored input noise [31] or by adjusting the fiber to attenuate the spectral components that might produce RS [18].

In studies of RS, a spectral filter is often applied to the supercontinuum. This selects only the long-wavelength extreme of the spectrum where RS are prominent, and allows the corresponding intensities to be identified [16,19]. This approach distinguishes the highly red-shifted RS from other intense features such as soliton collisions, but has two weaknesses. First, a suitable cut-on wavelength must be found which passes RS while suppressing the main body of the supercontinuum spectrum. Provided such a threshold is set, the histogram of peak transmitted intensities is characteristically "L-shaped" and RS can be readily identified as the features comprising the high-intensity tail [19]. However, filtering at too-short a wavelength transmits a quasi-Gaussian histogram in which the RS are not clearly distinguishable. A too-long wavelength filter may not fully capture the energy of RS and thus distorts the observed RS intensities [20]. Second, a fixed filter wavelength is therefore appropriate for identifying RS only at a fixed position (or over a limited range) along the fiber. That is because the supercontinuum spectrum broadens during propagation along the PCF. Hence a filter wavelength suitable for identifying RS at one fiber length is inappropriate for studying RS further along the fiber. This second issue is addressed in this work.

We present an adaptive spectral filter, which applies a fiber-length dependent cut-on wavelength. This filtering method identifies RS in a set of simulated supercontinua, and does so along the length of the fiber. Tracking individual RS along the fiber in this way reveals that they exhibit a lifecycle: they rapidly accumulate intensity and then slowly decline. As a consequence, highly intense RS will eventually be overtaken by newly-formed RS. This behavior has implications for the design of spectrally stable SC light sources.

2. Numerical model

The conversion of 1000 laser pulses to supercontinuum light in a PCF was simulated by numerically solving the generalized nonlinear Schrödinger equation (GNLSE) [1,2,32], Eq. (1).

$$\frac{\partial A}{\partial z} - \sum_{k\geq 0} \frac{i^{k+1}}{k!} \beta_k \frac{\partial^k A}{\partial T^k} = i\gamma\left(1 + i\tau_{shock} \frac{\partial}{\partial T}\right)\left(A(z,T) \int_{-\infty}^{+\infty} R(t') \left| A(z,T-t') \right|^2 dt' \right) \quad (1)$$

Where $A(z,T)$ is the time domain field envelope, $T = t - \beta_1 z$ is the retarded time traveling at the group velocity of the pump, and z is the propagation distance. Our simulations employ the fourth-order Runge-Kutta in the interaction picture (RK4IP) algorithm [33,34], using 16384 points in a time-grid of 80 ps. The input pulses were set to an unchirped hyperbolic secant form, with a center wavelength of 1060 nm, peak power P_0 = 100 W and width T_0 = 2.84 ps corresponding to 5 ps full width half maximum. Random noise was modeled by adding a single, random-phase photon per frequency bin to the input pulse [35]. The dispersion coefficients, β_k up to tenth order, and the other fiber parameters, were duplicated from a study by Dudley *et al*. [18], describing a PCF with a single zero dispersion wavelength at 1055 nm. The nonlinear coefficient, $\gamma(\omega_0)$ is 15/(W km). We use a detailed form of the

#136335 - $15.00 USD Received 8 Oct 2010; revised 19 Nov 2010; accepted 19 Nov 2010; published 30 Nov 2010

nonlinear response function $R(t)$ with f_R = 0.245 [36]. The dispersion of the nonlinearity is characterized by τ_{shock} with a value of 0.66 fs. In the near-infrared wavelengths of interest the attenuation is relatively low so that absorption was neglected.

3. Simulation results

3.1 Optical rogue waves

Figure 1 shows the spectra of 1000 simulated SC pulses overlaid together with their mean after a 26 m long PCF. Occasional SC pulses contain a spectral feature that is red-shifted far beyond the mean extent, as seen in many RS studies [18,19,22]. Two such outliers are highlighted and labeled as rogue solitons, RS-A and RS-B. These two features (circled in Fig. 1 (b)) exhibit almost identical red-shifts but disparate energy and filtered peak intensities (Fig. 2(a)). This difference depends on their distinct propagation along the fiber, which provides the motivation for the current study.

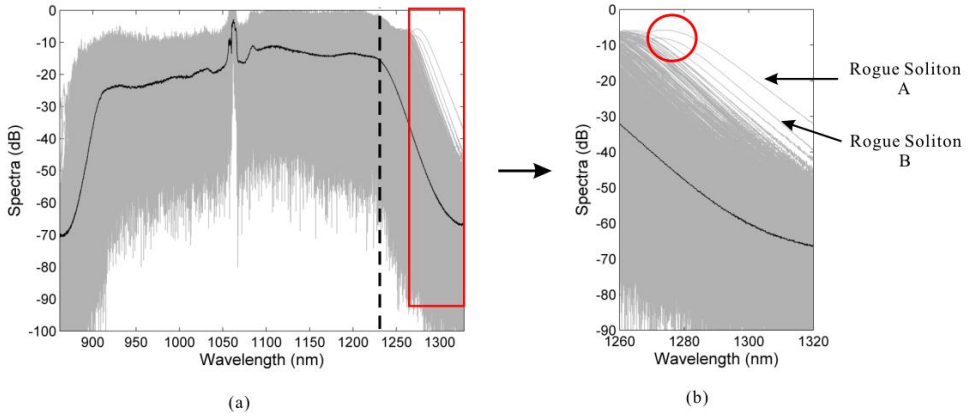

Fig. 1. (a) 1000 individual spectra (gray lines) at 26 m fiber length, the mean spectrum (black line), and the wavelength of a fixed cut-on filter (dotted line at 1237 nm). (b) Detail of the 1260 nm to 1320 nm range.

To characterize rogue solitons, they must first be sorted from the body of their SC pulse. A popular method is to apply a fixed spectral filter to each pulse [16,18–20]. The mean SC spectrum in Fig. 1 declines to −15 dB versus the residual pump power at 1237 nm wavelength. This is found to be a good rejection threshold to identify RS, in SC pulses generated using the parameters studied here. A fixed cut-on filter is applied at 1237 nm: this step-function numerical filter fully passes longer wavelength components, and stops others. The filtered spectra are Fourier transformed to determine the time-domain properties of features in the long-wavelength tail. Figure 2 presents the distribution of peak intensities and associated time-delays of these spectral outliers. Features in the high-intensity tail of the L-shaped intensity distribution are identified as RS [16–23].

Figure 2(b) shows that the spectral outliers have a positive correlation between intensity and mean time-lag. This trend is expected, since higher intensity solitons experience more efficient Raman scattering, undergo more red-shift, and accumulate greater dispersive time-lag. RS-B lies on the trend of intensity-delay. The most intense outlier, RS-A, has almost equal red-shift but its time-delay is below trend. This suggests an explanation: RS-A may have formed just shortly before the fiber position under analysis (26 m), and has not yet accumulated enough dispersive time delay to place it near-trend. To address length-dependent aspects of RS formation and subsequent evolution, rogue solitons need to be tracked along the fiber.

#136335 - $15.00 USD Received 8 Oct 2010; revised 19 Nov 2010; accepted 19 Nov 2010; published 30 Nov 2010

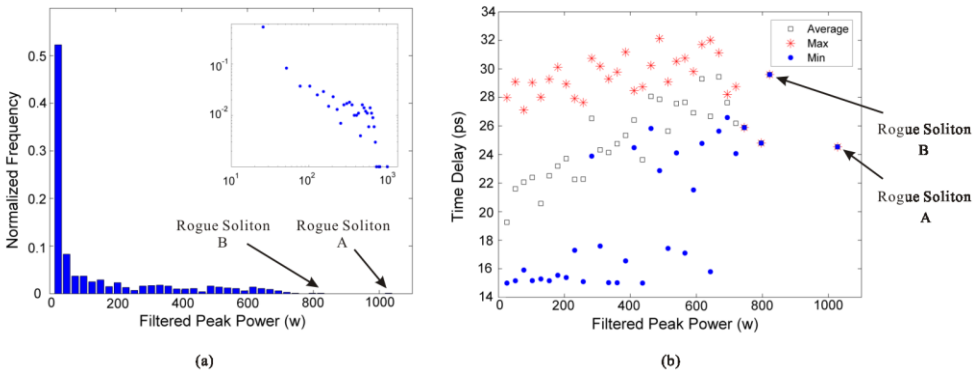

Fig. 2. (a) Histogram of numerically filtered peak powers. The inset shows the histogram on a log-log scale. (b) Average, maximum and minimum intra-pulse delay times of solitons in each power bin. The cut-on wavelength of the spectral filter was 1237 nm and the PCF length was 26 m. The peak powers and intra-pulse time delays of soliton A and B are 1027 W, 847 W, 24.5 ps and 29.6 ps, respectively.

3.2 Qualitative observation of RS evolution

Figure 3 shows the temporal and spectral evolution of selected SC pulses as a function of fiber length, and the corresponding spectrograms after 26 m of fiber. Figures 3 (a)-3(c) shows a pulse close to the mean spectral distribution. Figures 3(d)-3(f) and (g-i) illustrate the SC pulses that produce the optical rogue waves RS-A and RS-B respectively. These highly-intense solitons initially accumulate energy as a result of collisions. They then undergo Raman self frequency shift, and are ejected from the main body of the SC pulse due to their slower group velocity. The fiber position at which an RS separates from the main pulse body is significant, because it is only until this point that it can capture energy by soliton collisions. Subsequently the RS can only lose energy by Raman scattering, and its intensity also may also decline owing to temporal broadening caused by positive third order dispersion and decreasing nonlinearity. Separation positions, which can be identified as the final positions in the fiber where the RS collides with another soliton, are highlighted by dashed lines in Fig. 3 for RS-A and RS-B. Since RS-A separates from its pulse after a longer fiber length, it is perhaps unsurprising that it exhibits greater energy when compared with RS-B at a subsequent fiber position. It seems likely that RS-A has either captured more energy, or that it has declined for a shorter period.

Fiber-length dependence of RS is an interesting issue that should be considered in the design of supercontinuum light sources for spectroscopy. RS are a striking source of variation between SC pulses near the spectral edges of SC light. They directly affect the long wavelength edge of the SC spectrum, and the dispersive waves trapped by RS are also known to affect the short wavelength edge [20] (trapped dispersive waves are seen in the spectrograms in Fig. 3 at wavelengths around 900 nm and at time-delays behind the RS). The purpose of the adaptive filter that follows is therefore to study the number and intensities of RS over a range of fiber positions, within a large set of SC simulations.

#136335 - $15.00 USD Received 8 Oct 2010; revised 19 Nov 2010; accepted 19 Nov 2010; published 30 Nov 2010

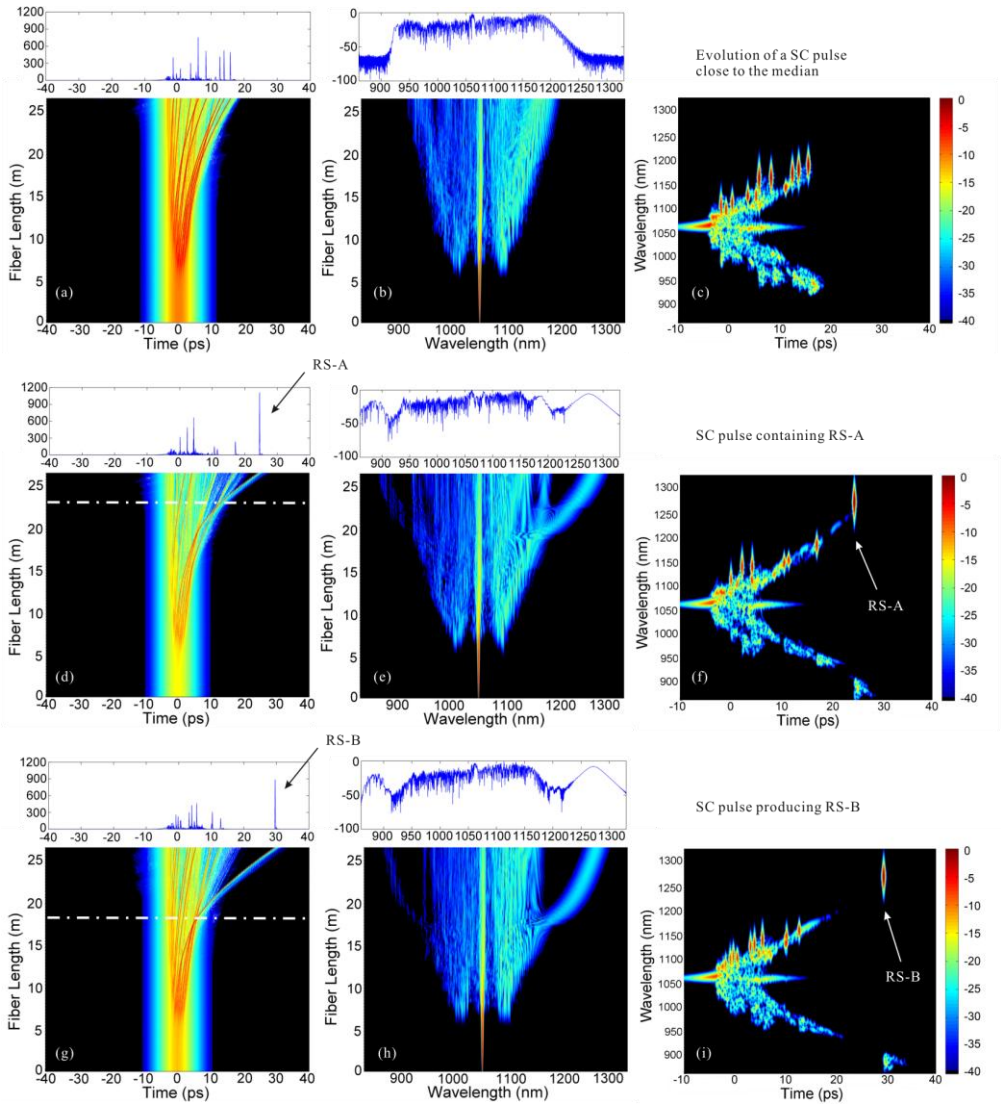

Fig. 3. Temporal (left) and spectral (middle) evolution of three SC pulses over a 26 m long PCF, and the corresponding spectrograms (right) at 26 m, with dB scales. (a-c) An SC pulse close to the mean spectral distribution, (d-f) pulse containing a rogue soliton, and (g-i) a pulse containing a rogue soliton that separates from its pulse at an earlier fiber position (dashed lines).

3.3 An adaptive spectral filter

A useful adaptive filter is obtained by taking a known spectral filtering method, which was applied and illustrated in Fig. 2, but replacing the fixed cut-on wavelength with a fiber-length dependent cut-on wavelength. The cut-on wavelength increases with propagation distance along the fiber, to account for spectral broadening of the supercontinuum light. It is important to set the cut-on wavelength in a systematic fashion. The fixed filter method set the cut-on wavelength at the position where the mean SC spectrum declines to −15 dB versus the residual pump. Hence we extend this method by setting a fiber-length dependent cut-on wavelength which traces the −15 dB position on the long wavelength side of the mean spectrum, as shown in Fig. 4. Cut-on wavelengths determined by the −15 dB position were

#136335 - $15.00 USD Received 8 Oct 2010; revised 19 Nov 2010; accepted 19 Nov 2010; published 30 Nov 2010

found to be effective for the identification of RS generated using the fiber parameters studied here.

Other adaptive filter thresholds were compared with the −15 dB level. For this data set the −10 dB level did not track the edge of the mean SC spectrum, and was unsuitable for identifying RS. Filters set at −20 dB or lower transmitted the same RS identified by the −15 dB filter, but only partially captured some of these, so the −15 dB level was preferred. For all these thresholds, the traced cut-on wavelengths increase stepwise at a fiber length where four-wave mixing first generates significant spectral sidebands. For the −15 dB filter this occurs at about 10 m. This is the position where long-wavelength features begin to emerge, so filtered data are presented from here onwards.

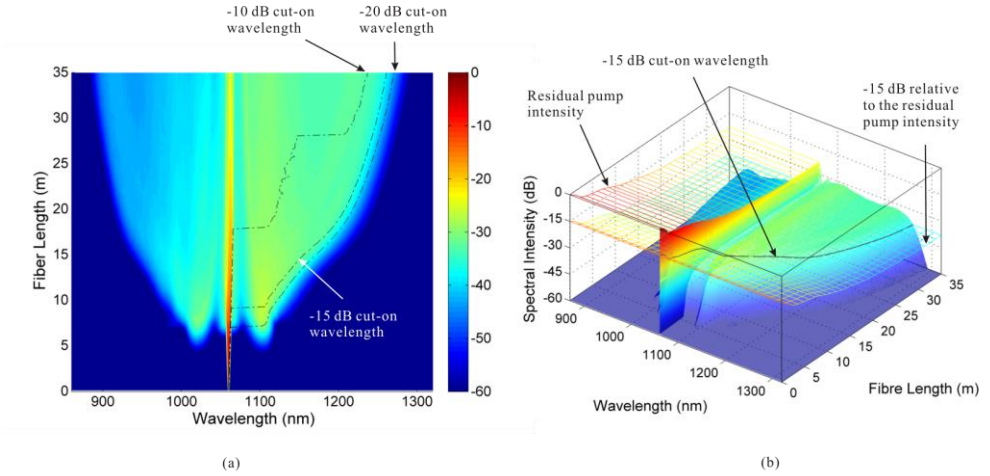

Fig. 4. (a) Mean spectrum of 1000 supercontinuum simulations, and the −10 dB, −15 dB and −20 dB edges along a 35 m fiber. (b) Plot showing determination of the −15 dB cut-on wavelength by the intersection of the −15 dB surface with surface of the mean spectrum.

3.4 Observing RS evolution by adaptive filtering

The adaptive numerical filter was applied to the SC pulse data set with results shown in Fig. 5. L-shaped intensity histograms, which are characteristic of RS dynamics, are identifiable over a wide range of fiber positions. The fiber-length dependence of the long-tailed intensity distributions can thus be studied. Individual RS can be distinguished by selecting features in the tails of these distributions, so the evolving properties of specific RS, i.e. their life cycle, can also be studied. This is possible, because individual outliers identified in the frequency domain can be uniquely correlated to features in the time domain. Thus any entry that can be distinguished in the L-shaped histogram distribution can be traced in the time domain from the pulse simulation that produced this entry. The properties of that RS can then be studied at other fiber positions by analyzing that particular pulse simulation with the adaptive spectral filter. It is this combination of studying RS properties both in the spectral and temporal domains that empowers our method, and permits the life cycle of RS to be investigated. This is shown in Fig. 5(a), where two specific rogue solitons are highlighted among the filtered intensity distributions, and their development at various fiber positions is plotted. In Fig. 5(b), the intensities captured by the adaptive filter are shown for four specific pulse simulations and seen to rise and decline with fiber position. From these pulses it is evident that RS are generated at various fiber positions: among the four pulses shown, a rapid intensity increase, i.e. formation of a RS, is seen to occur at different fiber positions, followed by slow decline. However, a problem with spectral filtering is that a part of the soliton energy spectrum may be lost. One must therefore be careful in interpreting the evolution of soliton properties using

#136335 - $15.00 USD Received 8 Oct 2010; revised 19 Nov 2010; accepted 19 Nov 2010; published 30 Nov 2010

only data thus filtered. However, here we also propose to use the adaptive spectral filter to identify the position of the RS in the time-domain as a function of fiber length. Once the position of a RS is known, it can be studied in the unfiltered data.

The long-tailed intensity distribution, shown in Fig. 5(a), is identified by adaptive filtering at a wide range of fiber positions. Although this distribution persists along the fiber length, the intensities of individual RS vary widely within it. Typical rogue solitons are highlighted: RS-A and RS-B. Both RS arise suddenly at a certain fiber position (as seen from Fig. 5(b)) although their intensities at earlier fiber positions are unremarkable. From the traces in Fig. 5(b) there is evidence that the RS then decline as they propagate along the fiber, and this seems to be a general characteristic of rogue solitons. However, since some information is sacrificed when spectral filtering methods are applied, it is useful to analyze the characteristics of corresponding features in the unfiltered intensity data. This analysis is presented in Fig. 5(c). Clearly the unfiltered data contain frequent spikes that are weak or absent in the corresponding filtered traces in Fig. 5(b). The spikes identify collisions with other solitons, which are excluded by spectral filtering. The unfiltered data thus contain information on soliton collisions, which are one of the main mechanisms leading to RS formation. It can be seen that prominent peaks in the unfiltered intensity data always precede the identification of rogue solitons in the filtered data. The filtered intensities rise smoothly following these events. This suggests that the collisions produce highly intense solitons, and during further propagation these features become remarkably red-shifted. This is consistent with the description of RS formation presented in [18] and [37]. The RS tracked in Fig. 5 seem to experience few collisions at fiber positions beyond 25 m. In this region of long propagation distances, the unfiltered intensities of RS clearly exhibit the same slow decline that was identified by the adaptive filter. This provides evidence that the decline of RS is not an artifact of spectral filtering.

It has been suggested that the sudden formation of RS is caused by turbulent collisions [19]. The subsequent decline, however, reflects two new aspects relating to SC propagation along fibers. The first aspect is that the absolute intensity of an RS decreases slowly after it separates from the body of its SC pulse. This decrease can be positively identified in the unfiltered intensities of the RS. These observations support the notion that rogue solitons experience energy loss due to Raman scattering, and temporal broadening due to positive third order dispersion and decreasing nonlinearity, which lead to a slow decrease in intensity. A second aspect is that RS which arise after long propagation lengths have had greater opportunity to gain energy from soliton collisions. This means therefore, that existing RS tend to be surpassed by newer RS which arise at subsequent fiber positions. Because RS arise rapidly but decline slowly, and because RS can arise at different positions along the fiber, the number of RS rises with increasing fiber length. This has consequences for the design of spectroscopic light sources: SC light generated in longer fibers contains a greater number of mature, declining rogue solitons. These outliers are responsible for significant instabilities near the edges of the emitted SC spectra. Controlling this spectral variation is a challenging task, but it is important to the design of stable light sources. One promising method for controlling RS, and one which takes account of their fiber-length dependence, is the sliding frequency fiber-grating filter proposed by Dudley [18].

Observing the rise and slow decline of RS offers insight into their eventual fate at large propagation distances. It has been suggested that RS may eventually collapse due to cumulative Raman scattering [16]. Other numerical studies reported that RS always retain their distinct structure until the end of the simulated fiber [19]. Our analysis confirms that RS propagating in fibers do not undergo sudden collapse. Rather, RS remain identifiable as distinctive outliers within the L-shaped intensity distributions (although they decline slowly within this distribution). The ability to observe the properties of rogue solitons over a wide range of fiber positions is the significant advantage of the adaptive spectral filter.

#136335 - $15.00 USD Received 8 Oct 2010; revised 19 Nov 2010; accepted 19 Nov 2010; published 30 Nov 2010

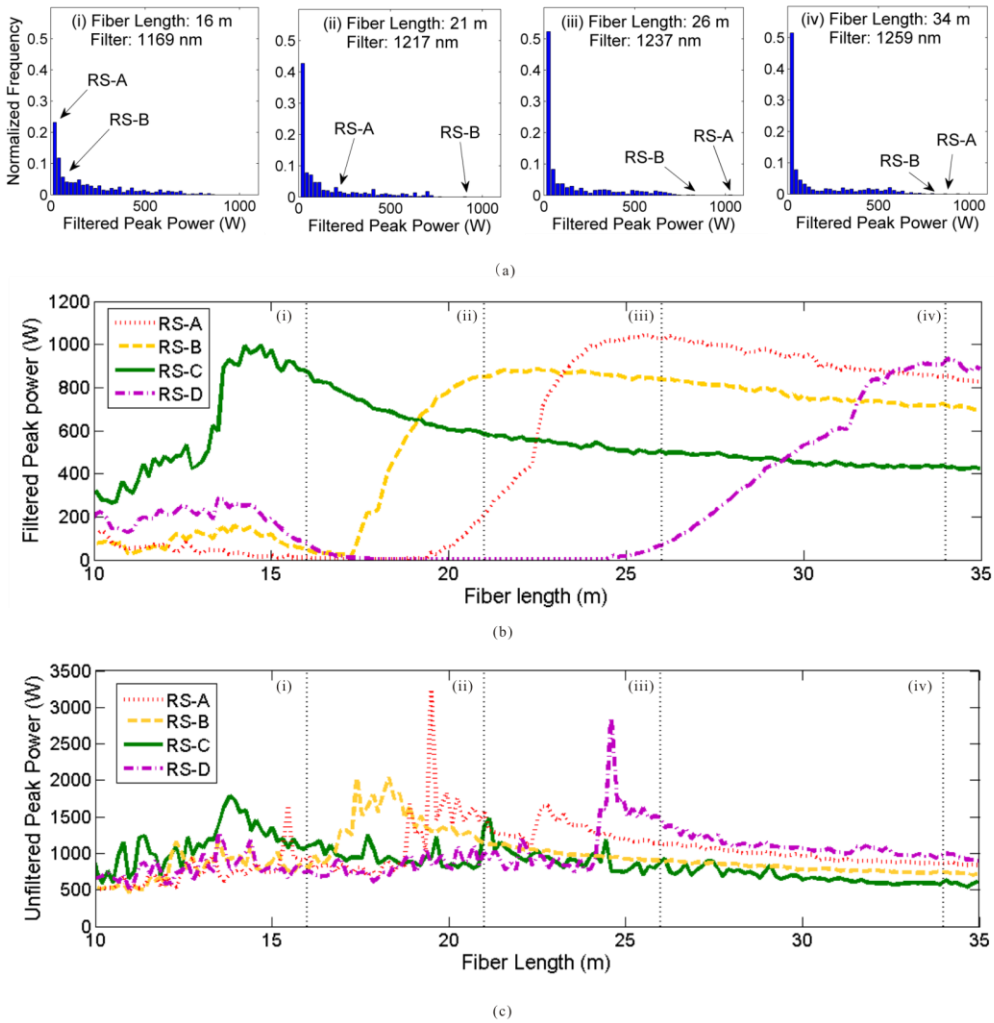

Fig. 5. (a) Adaptive spectral filtering identifies L-shaped intensity histograms over a wide range of positions along the fiber. (b) The filter permits easy identification of rogue solitons, which appear as rapid intensity rises at certain fiber positions. (c) The corresponding unfiltered properties of the same rogue solitons can also be tracked. Sharp peaks are seen on these traces, identifying soliton collision events. It is seen that RS formed, arise quickly in time, but decline slowly. These properties are also presented dynamically (Media 1).

4. Conclusions

Rogue solitons were identified in a set of supercontinuum simulations performed using the RK4IP algorithm. An adaptive numerical filter was developed which accounts for ongoing spectral broadening of SC pulses, and captures unusually red-shifted features along the entire length of a fiber. The adaptive filter identifies the long-tailed intensity distributions associated with RS at all fiber positions subsequent to the onset of modulation instability; however the properties of individual RS within this distribution vary with fiber length. Rogue solitons have a lifecycle: they are suddenly formed by accumulation of energy from collisions, and then they slowly decline. Declining RS retain significant intensity, but can always be surpassed by newly-formed RS. Since RS cause significant intensity variations at the spectral edges of generated supercontinuum light, an understanding and control of RS behavior is required in the design of stable light sources.

#136335 - $15.00 USD Received 8 Oct 2010; revised 19 Nov 2010; accepted 19 Nov 2010; published 30 Nov 2010

Acknowledgement

This work was funded by EPSRC grants (EP/G04690 and EP/F028261). The research leading to these results has received funding from the European Community's Seventh Framework Programme (FP7/2007-2013) under grant agreement no PIEF-GA-2008-221538. Chu Liu is supported by the China Scholarship Council. The authors thank Dr. Johan Hult for his support and advice.

#136335 - $15.00 USD Received 8 Oct 2010; revised 19 Nov 2010; accepted 19 Nov 2010; published 30 Nov 2010